

IEKP-KA/2000-23

hep-ph/0007078

**The $b \rightarrow X_s \gamma$ decay rate in NLO,
Higgs boson limits, and LSP masses in the Constrained
Minimal Supersymmetric Model**

W. de Boer, M. Huber

*Institut für Experimentelle Kernphysik, University of Karlsruhe
Postfach 6980, D-76128 Karlsruhe, Germany*

A.V. Gladyshev, D.I. Kazakov

*Bogoliubov Laboratory of Theoretical Physics, Joint Institute for Nuclear
Research,
141 980 Dubna, Moscow Region, Russian Federation*

Abstract

New NLO $b \rightarrow X_s \gamma$ calculations have become available. We observe that at large $\tan \beta$ the dominant NLO term of the chargino amplitude, which is proportional to $\mu \tan^2 \beta$, changes the sign of this amplitude in a large region of the CMSSM parameter space, so that the preferred sign of the Higgs mixing parameter μ now agrees with the preferred sign of $b - \tau$ unification. We find that the $b \rightarrow X_s \gamma$ rate does not constrain the CMSSM anymore, if the higher order contributions and its uncertainties from the incomplete calculations are taken into account.

The Higgs boson mass in the CMSSM is found to be between 110 and 120 GeV for a top mass of 175 GeV, if the Higgs mass limit of 107.9 GeV from LEP, which implies $\tan \beta > 3.3$, is taken into account. The mean Higgs boson mass value and its dominant errors are: $m_h = 115 \pm 3$ (stopmass) ± 1.5 (stopmixing) ± 2 (theory) ± 5 (topmass) GeV. This Higgs mass range is valid for all $\tan \beta$ values above 20 and decreases for lower $\tan \beta$.

If the presently claimed evidence for dark matter by the DAMA Collaboration is interpreted as the Lightest Supersymmetric Particle (LSP) of the CMSSM, then it is at the edge of the parameter space allowed by the present Higgs limit of 107.9 GeV from LEP.

1 Introduction

In a previous paper we showed that the inclusive decay rate $b \rightarrow X_s \gamma$ severely constrains the high $\tan \beta$ solution of the Constrained Minimal Supersymmetric Standard Model (CMSSM) [1]. This was mainly caused by the fact that $b - \tau$ Yukawa coupling unification preferred a negative sign for the Higgs mixing parameter μ , while the $b \rightarrow X_s \gamma$ rate required the opposite sign. However, with the advent of next-to-leading order (NLO) calculations for the $b \rightarrow X_s \gamma$ rate in the MSSM [2] it turns out that large terms proportional to $\tan^2 \beta$ can change the sign of μ . Consequently the allowed parameter space becomes much larger for the high $\tan \beta$ scenario, especially if the uncertainties from the incomplete NLO calculations are taken into account in our global analysis.

Here we used the $b \rightarrow X_s \gamma$ rate from the CLEO Collaboration, as presented at the Stanford Lepton-Photon '99 Conference [3]: $BR(b \rightarrow X_s \gamma) = (3.15 \pm 0.35 \pm 0.32 \pm 0.26) \cdot 10^{-4}$. This value combined with the less precise ALEPH measurement [4] of $BR(b \rightarrow X_s \gamma) = (3.11 \pm 0.80 \pm 0.72) \cdot 10^{-4}$ yields as average $BR(b \rightarrow X_s \gamma) = (3.14 \pm 0.48) \cdot 10^{-4}$

The present SM Higgs limit of 107.9 GeV[5] puts severe constraints on the CMSSM parameter space, since in the CMSSM the heavier Higgs decouple, so the lightest Higgs has the properties of a SM Higgs. These constraints, as well as the chargino limits from LEP[6], are compared with the recently claimed evidence by the DAMA Collaboration[7] for dark matter, which can be interpreted in the CMSSM as a stable neutralino with a mass of 52_{-8}^{+10} GeV.

2 Numerical analysis method

Our statistical analysis of the allowed parameter space in the MSSM[1] was repeated including the new partial NLO $b \rightarrow X_s \gamma$ calculations. In this χ^2 analysis the constraints from gauge coupling unification, $b - \tau$ Yukawa coupling unification, electroweak symmetry breaking, $b \rightarrow X_s \gamma$, relic density and experimental lower limits on SUSY masses can be considered either separately or combined. In this paper we do not include constraints from relic density, which are relevant mainly at low $\tan \beta$.

As free parameters of the Constrained MSSM (CMSSM) we consider the unified gauge coupling constant (α_{GUT}) at the unification scale (M_{GUT}). In addition we define at the GUT scale: the Yukawa coupling constants of the third generation (Y_t^0, Y_b^0, Y_τ^0), the common scalar mass (m_0), the common gaugino mass ($m_{1/2}$), the common trilinear coupling ($A_t^0 = A_b^0 = A_\tau^0$), the ratio of the vacuum expectation values of the two Higgs doublets ($\tan \beta$), the Higgs mixing parameter μ^0 . The GUT scale parameters are optimized via a χ^2 test to fit the low energy experimental data on electroweak boson masses, $b \rightarrow X_s \gamma$, and quark and lepton masses of the third generation.

The values of m_0 , $m_{1/2}$, μ^0 , A^0 , Y^0 and $\tan\beta$ determine completely the mass spectrum of all SUSY particles via the RGE. The values of μ^0 , Y^0 and $\tan\beta$ are constrained for given values of m_0 and $m_{1/2}$ by EWSB and the quark and lepton masses of the third generation. Since m_0 and $m_{1/2}$ are strongly correlated, we repeat each fit for every pair of m_0 and $m_{1/2}$ values between (200,200) and (1000,1000) GeV in steps of 100 GeV.

As can be seen from Fig. 1 the value of $\tan\beta$ is constrained by the present experimental value of the top mass $m_t = 173.9 \pm 5.2$ GeV[8] to be in the following ranges: $1 < \tan\beta < 2$ or $30 < \tan\beta < 40$ for $\mu < 0$. These constraints result mainly from the $b - \tau$ Yukawa unification. In the following we will first concentrate on these $\tan\beta$ values, which we call the low and high $\tan\beta$ scenario, but consider the complete $\tan\beta$ dependence as well.

3 NLO corrections to $b \rightarrow X_s \gamma$

The $b \rightarrow X_s \gamma$ transition corresponds in lowest order to a loop with either a W, charged Higgs or chargino, as shown schematically in Fig. 2. The leading order corresponds to the emission of a real photon from any of the charged lines, while the dominant next-to-leading order (NLO) corrections involve virtual gluons from any of the (s)quark lines,

The LO Standard Model (SM) calculations [9, 10, 11] have been complemented by NLO calculations [12, 13, 14, 15]. Recently, the NLO calculations have been extended to Two-Higgs Doublet Models (2HDM) [16, 17] and the Minimal Supersymmetric Model (MSSM) for a given mass hierarchy [2, 18].

Here we use the results from Ref. [2], which are valid for any value of $\tan\beta$. After studying the paper from Ref. [2] in detail[19], we found that the NLO corrections to the chargino amplitude have two main contributions: the first one is proportional to $\mu \tan\beta / \cos\beta$ (for large $\tan\beta \propto \tan^2\beta$) coming from the sbottom mixing (e.g. the last diagram in Fig.2), and the second one is proportional to large log terms $\sim \log \tilde{m}_g/\mu_W$ coming from diagrams with gluinos. (lowest row in Fig.2). The $\tan^2\beta$ dependence of the first term implies that these corrections are significant for the high $\tan\beta$ scenario discussed above. Note that the NNLO contributions do not have a $\tan^3\beta$, since the sbottom mixing comes in only once, so the series is converging rapidly afterwards, because of the $(\alpha_s/\pi)^2$ suppression.

The large NLO contributions change the sign of the chargino amplitude at large $\tan\beta$ for practically the whole parameter space, as shown in Fig. 3. Since the chargino-stop amplitude is of the same order of magnitude as the SM W-t amplitude for most of the parameter space, it interferes strongly: positively for $\mu > 0$ and negatively for $\mu < 0$. In the first case the $b \rightarrow X_s \gamma$ rate becomes rapidly too big for large $\tan\beta$, as shown in Fig. 4. Note the change in sign of μ for the positive (negative) interference between LO and NLO in the figure.

The scale dependence in NLO is still large, as shown by the width of the bands in Fig. 4, which may be related to the incomplete NLO calculations. Due to the large scale uncertainty one expects a good fit for practically all values of $\tan\beta$ and $\mu < 0$, if the scale is left free in the fit within the limits of 0.5 and 2 m_b . This is shown in Fig. 5, where only a very small corner is excluded by $b \rightarrow X_s \gamma$ in contrast to the previous LO calculations[1].

In Ref. [2] only the effect of the lightest stop to the NLO contributions was considered and no flavour mixing between the three generations was taken into account. The latter was found to be small in the CMSSM. The effect of the missing contributions of the heavier stop has been studied. The general picture does not change by including heavier stop terms analogous to the light stop terms, although complete calculations including diagrams where both stops contribute simultaneously have not yet been calculated. Given the uncertainties from the incomplete calculations, we will exclude hereafter the $b \rightarrow X_s \gamma$ constraint from the fit and study the Higgs mass prediction in the CMSSM.

4 Higgs mass predictions

In Supersymmetry the couplings in the Higgs potential are the gauge couplings. The absence of arbitrary couplings together with well defined radiative corrections to the masses results in clear predictions for the lightest Higgs mass and electroweak symmetry breaking (EWSB).

In the Born approximation one expects the lightest Higgs to have a mass m_h below the Z^0 mass. However, loop corrections, especially from top and stop quarks, can increase m_h considerably. The Higgs mass depends mainly on the following parameters: the top mass, the squark masses, the mixing in the stop sector, the pseudoscalar Higgs mass and $\tan\beta$. As will be shown below, the maximum Higgs mass is obtained for large $\tan\beta$, for a maximum value of the top and squark masses and a minimum value of the stop mixing. The Higgs mass calculations were carried out following the results obtained by Carena, Quirós and Wagner[21] in a renormalization group improved effective potential approach, including the dominant two-loop contributions from gluons and gluinos.

Note that in the CMSSM the Higgs mixing parameter μ is determined by the requirement of EWSB, which yields large values for μ [20]. Given that the pseudoscalar Higgs mass increases rapidly with μ , this mass is always much larger than the lightest Higgs mass and thus decouples. We found that this decoupling is effective for all regions of the CMSSM parameter space, i.e. the lightest Higgs has the couplings of the SM Higgs within a few percent. Consequently the experimental limits on the SM Higgs can be taken.

The lightest Higgs boson mass m_h is shown as function of $\tan\beta$ in Fig. 6. The shaded band corresponds to the uncertainty from the stop mass and stop mixing for $m_t = 175$ GeV. The upper and lower lines correspond to $m_t = 170$ and 180

GeV, respectively.

One observes that for a SM Higgs limit of 107.9 GeV [5] all values of $\tan \beta$ below 3.3 are excluded in the CMSSM.

In order to understand better the Higgs mass uncertainties, the relevant parameters were varied one by one. The Higgs mass varies between 110 and 120 GeV, if m_0 and $m_{1/2}$ are varied between 200 and 1000 GeV, which implies stop masses varying between 400 and 2000 GeV, as shown in Fig. 7. Since at present there is no preference for any of the values between 110 and 120 GeV, the variance for a flat probability distribution is $10/\sqrt{12}=3$ GeV, which we take as an error estimate.

The dependence of the Higgs mass on A_0 is shown in Fig. 8 for the high $\tan \beta$ scenario. The influence on the Higgs mass is quite small in the CMSSM, since the low energy value A_t tends to a fixed point, so that the stop mixing parameter $X_t = A_t - \mu/\tan \beta$ is not strongly dependent on A_0 . Furthermore, the μ term is not important at large $\tan \beta$. If we vary A_0 between $\pm 3m_0$, the the error from the stop mixing in the Higgs boson mass is estimated to be ± 1.5 GeV. The values of $m_0 = m_{1/2} = 370$ GeV yield the central value of $m_h = 115$ GeV.

The dependence on m_t is shown in Fig. 9 for $A_0 = 0$ and intermediate values of m_0 and $m_{1/2}$ for two values of $\tan \beta$ (corresponding to the minimum χ^2 values in Fig. 1). The uncertainty from the top mass at large $\tan \beta$ is ± 5 GeV, given the uncertainty on the top mass of 5.2 GeV.

The uncertainties from the higher order calculations (HO) is estimated to be 2 GeV from a comparison of the full diagrammatic method [22] and the effective potential approach[21], so combining all the uncertainties discussed before we find for the Higgs mass in the CMSSM

$$m_h = 115 \pm 3 \text{ (stopmass)} \pm 1.5 \text{ (stopmixing)} \pm 2 \text{ (theory)} \pm 5 \text{ (topmass)} \text{ GeV.}$$

where the errors are the estimated standard deviations around the central value. As can be seen from Fig. 6 this central value is valid for all $\tan \beta > 20$ and decreases for lower $\tan \beta$.

5 Higgs and Chargino mass versus LSP mass

In the CMSSM considered here all masses are related, since they have a common mass at the GUT scale. The low energy values are completely determined by the renormalization group equations[20]. If R-parity is conserved, the lightest supersymmetric particle (LSP) will be stable, which is usually the lightest neutralino. This LSP has all the properties of a WIMP (Weakly Interacting Massive Particle) required for the cold dark matter in our universe.

The contours of the Higgs mass, chargino mass and LSP mass are shown in Fig. 10. The LSP is practically independent of m_0 and is given by $\approx 0.4m_{1/2}$ [20], so an LSP of 52_{-8}^{+10} which could be the interpretation of the annual modulation

signature observed by the DAMA Collaboration[7], corresponds to $m_{1/2} \approx 130^{25}_{20}$ GeV. As can be seen from Fig. 10, the central value of 130 GeV is excluded by a Higgs mass below 107.9 GeV for m_0 below 750 GeV and for a chargino mass below 100 GeV for the higher m_0 values.

For this year of LEP running one hopes to be sensitive to Higgs masses up to 114 GeV, i.e. LSP masses up to 120 GeV, which clearly will be able to answer the question, if the observation by the DAMA collaboration can be interpreted as a CMSSM LSP.

6 Conclusions

The results can be summarized as follows:

- The NLO $b \rightarrow X_s \gamma$ contributions change the preferred sign of the Higgs mixing parameter μ for the large $\tan \beta$ scenario of the CMSSM. Since this sign agrees now with the sign preferred from $b - \tau$ unification, the allowed parameter becomes much larger. Given the larger uncertainties from the still incomplete calculations, we conclude that at present no constraints from $b \rightarrow X_s \gamma$ can be derived.
- The low $\tan \beta$ scenario ($\tan \beta < 3.3$) of the CMSSM is excluded by the lower limit on the Higgs mass of 107.9 GeV[5].
- For the high $\tan \beta$ scenario the Higgs mass is found to be in the range from 110 to 120 GeV for $m_t = 175$ GeV. The errors around the central value of 115 GeV are found to be: $m_h = 115 \pm 3$ (*stopmass*) ± 1.5 (*stopmixing*) ± 2 (*theory*) ± 5 (*topmass*) GeV. This prediction is independent of $\tan \beta$ for $\tan \beta > 20$ and decreases for lower $\tan \beta$.
- The interpretation of the annual modulation signature by the DAMA Collaboration as the lightest neutralino in the CMSSM is at the edge of the parameter space allowed by the present Higgs and chargino limits. Future running at LEP will be able to settle the question, if an LSP of 52^{+10}_8 GeV can be accommodated in the CMSSM.

Acknowledgements

We thank P. Gambino, G.F. Giudice and M. Misiak for helpful discussions on the NLO $b \rightarrow X_s \gamma$ rates.

References

- [1] W. de Boer, H.-J. Grimm, A.V. Gladyshev, D.I. Kazakov, Phys. Lett. **B 438** (1998) 281.
- [2] M. Ciuchini, G. Degrassi, P. Gambino, G.F. Giudice, Nucl. Phys. **B 534** (1998) 3-20.
- [3] Ronald Poling (University of Minnesota), Talk at the Lepton - Photon '99 Conference, Stanford University, USA, 9-14 August 1999; see also CLEO Collaboration, CLEO CONF 98-17, ICHEP98 1011.
- [4] R. Barate et al. (ALEPH Collaboration), Phys. Lett. **B 429** (1998) 169.
- [5] The LEP Higgs Working Group, R. Bock et al., CERN-EP-2000-055 and the LEP experiments, ALEPH 2000-28, DELPHI 2000-050, L3-Note 2525, OPAL TN646,
- [6] G. Ganis, talk at SUSY2000, CERN, Geneva, June 2000
- [7] R. Bernabei et al., Phys. Lett. **B480** (2000) 21
- [8] Particle Data book, Eur. Phys. J. **C3** (1998) 1.
- [9] B. Grinstein, R. Springer and M.B. Wise, Nucl. Phys. **B 339**, 269 (1990).
- [10] S. Bertolini, F. Borzumati, A. Masiero, G. Ridolfi, Nucl. Phys. **B 353** (1991) 591.
- [11] A.J. Buras, M. Misiak, M. Münz and S. Pokorski, Nucl. Phys. **B 424**, 374 (1994).
- [12] K. Adel and Y.P. Yao, Phys. Rev. **D 49**, 4945 (1994).
- [13] C. Greub and T. Hurth, Phys. Rev. **D 56**, 2934 (1997).
- [14] A. Ali and C. Greub, Phys. Lett. **B 361**, 146 (1995). A. Ali, C. Greub, Z.Phys. **C 60** (1993) 433.
- [15] C. Greub, T. Hurth and D. Wyler, Phys.Lett. **B 380**, 385 (1996); Phys. Rev. **D 54**, 3350 (1996).
- [16] M. Ciuchini, G. Degrassi, P. Gambino and G.F. Giudice, Nucl. Phys. **B 527** (1998) 21-43.
- [17] F.M. Borzumati and C. Greub, Phys. Rev. **D59** (1999) 57501.
- [18] C. Bobeth, M. Misiak, and J. Urban, TUM-HEP-321-98, hep-ph/9904413
- [19] M. Huber, Preprint IEKP-KA/2000-4, Diplomarbeit, Universität Karlsruhe.
- [20] See e.g. W. de Boer, Prog. Part. Nucl. Phys. **33**(1994) 201 and references therein.
- [21] M. Carena, M. Quirós and C. Wagner, Nucl. Phys. **B 461** (1996) 407
- [22] M. Carena et al., Nucl. Phys. **B580** (2000) 29

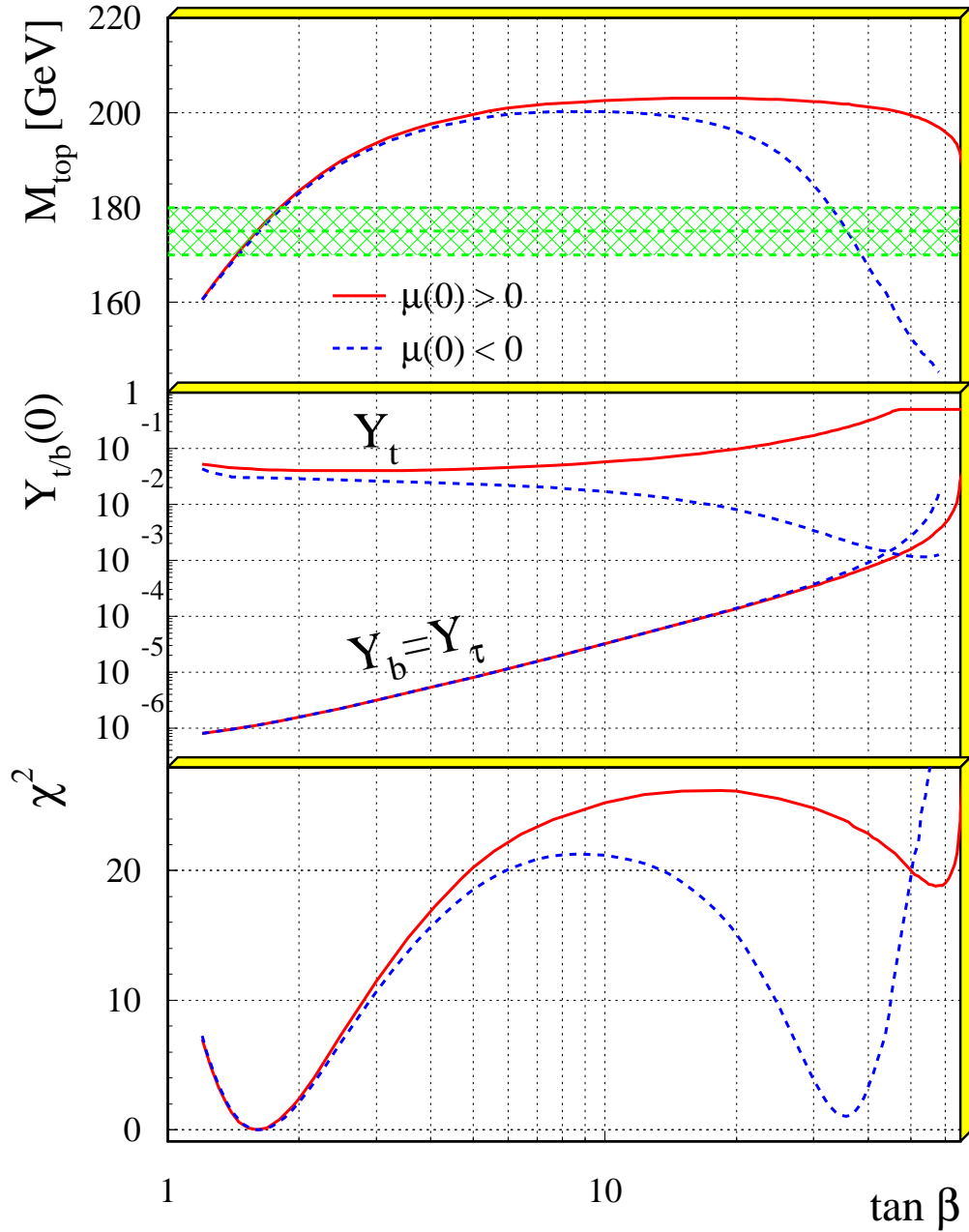


Figure 1: The upper part shows the top quark mass as function of $\tan \beta$ for $m_0 = 600$ GeV, $m_{1/2} = 400$ GeV. The middle part shows the corresponding values of the Yukawa couplings at the GUT scale and the lower part the χ^2 values. As can be seen the value of $\tan \beta$ is restricted to be in the following ranges $1 < \tan \beta < 2$ or $30 < \tan \beta < 40$ for $\mu < 0$.

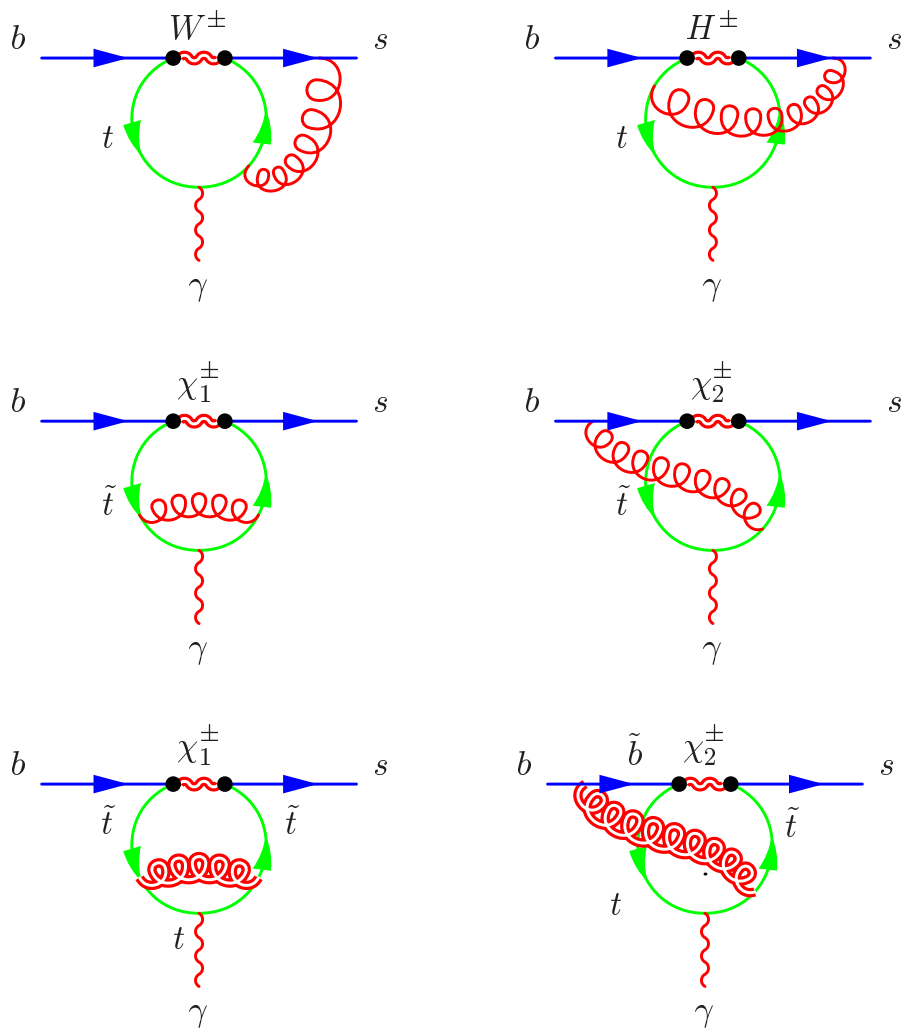


Figure 2: Some electroweak loop diagrams for the $b \rightarrow X_s \gamma$ transition in NLO.

$$\tan \beta = 35, \mu < 0$$

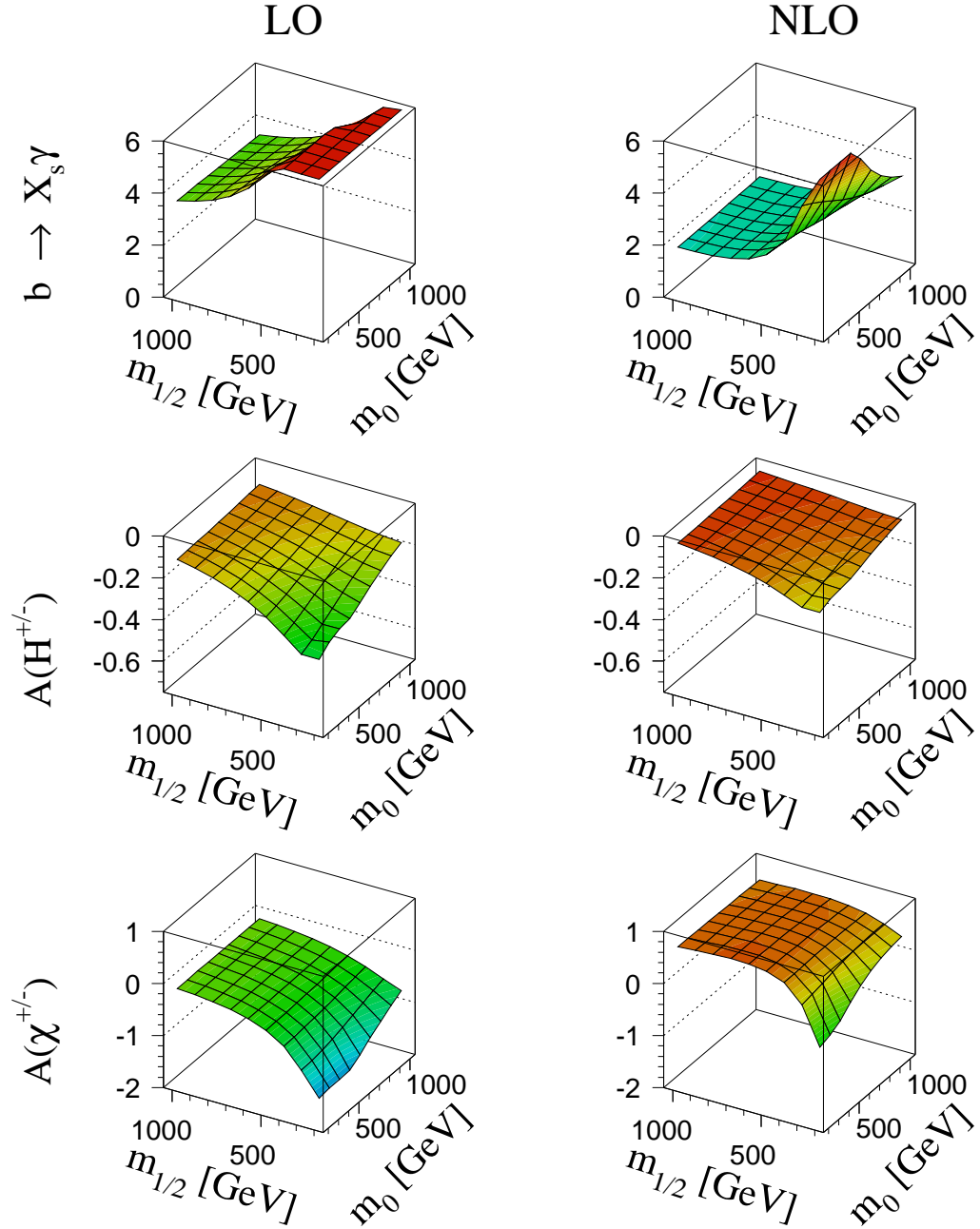


Figure 3: The decay rate (in units of 10^{-4}) and selected amplitudes (in units of 10^{-2}) of the $b \rightarrow X_s \gamma$ decay for negative μ and $\tan \beta = 35$. These amplitudes should be compared with the SM amplitude of $-0.56 \cdot 10^{-2}$. Note the sign change in the χ^\pm amplitude.

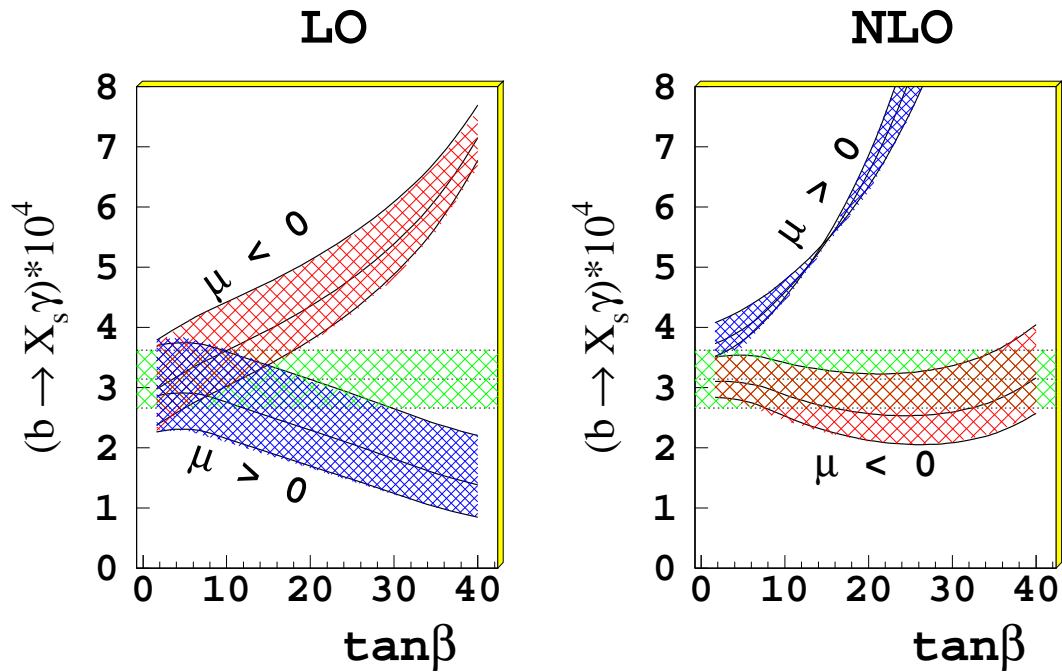


Figure 4: The dependence of the $b \rightarrow X_s \gamma$ rate on $\tan\beta$ for LO (l.h.s.) and NLO (r.h.s.) for $m_0 = 600$ GeV and $m_{1/2} = 400$ GeV. A fit was made for each value of $\tan\beta$ and μ . The curved bands show the theoretical prediction; its width is determined by the renormalization scale uncertainty, if this is varied between $0.5m_b$ and $2m_b$. The horizontal band shows the experimental value $\pm 1\sigma$.

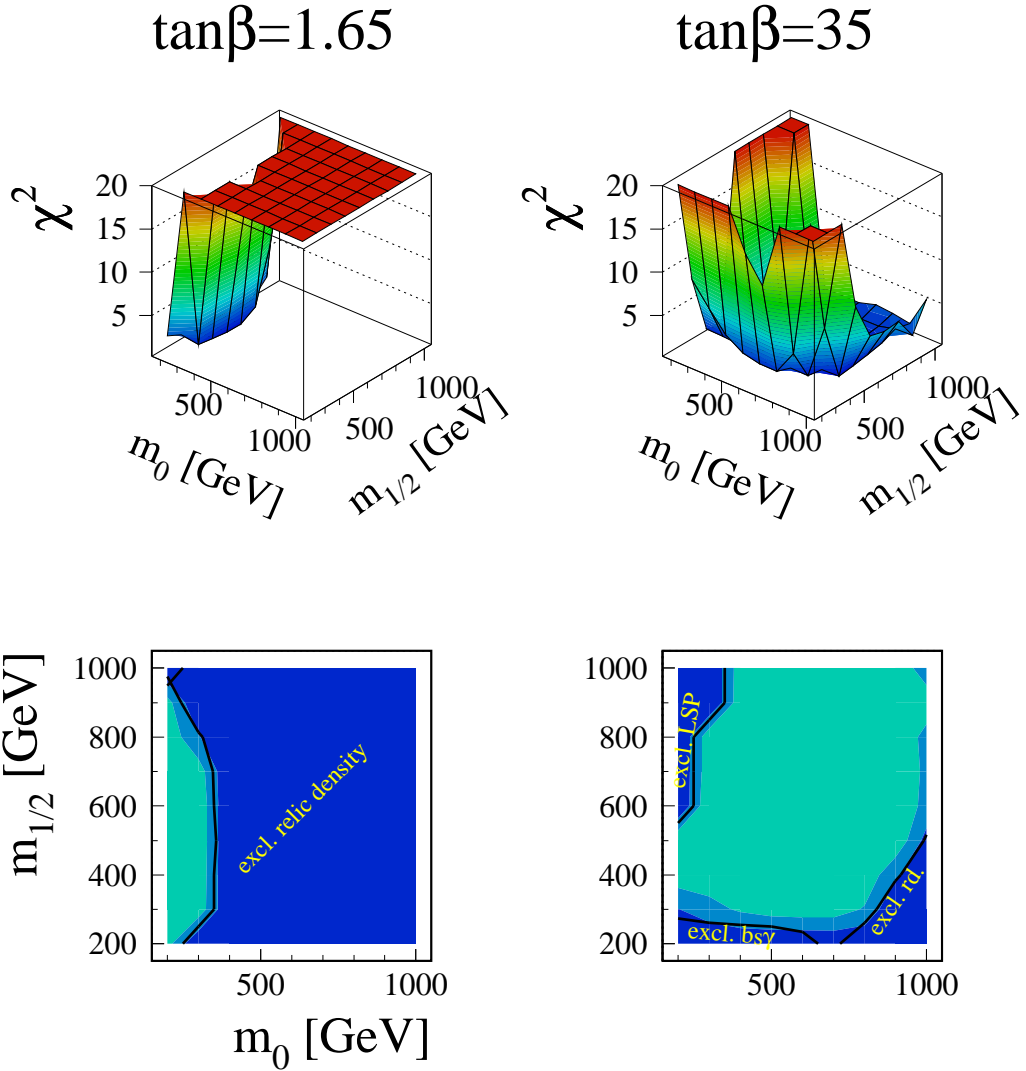


Figure 5: The upper row shows the χ^2 distribution in the $m_0 - m_{1/2}$ plane for $\tan\beta = 1.65$ and $\tan\beta = 35$. The projections are shown in the second row. The different shades in the projections indicate steps of $\Delta\chi^2 = 4$. The contour lines show areas excluded by the particular constraints used in the analysis: in the LSP area the Lightest Supersymmetric Particle is charged (usually the stau), which is not allowed if the LSP is stable, in the relic density (rd) area the density of the universe is above the critical density and in the $bs\gamma$ area the $b \rightarrow X_s \gamma$ rate is too high. In the $\tan\beta = 35$ plots the μ_b -scale was allowed to vary between $0.5m_b$ and $2m_b$ for the $b \rightarrow X_s \gamma$ rate.

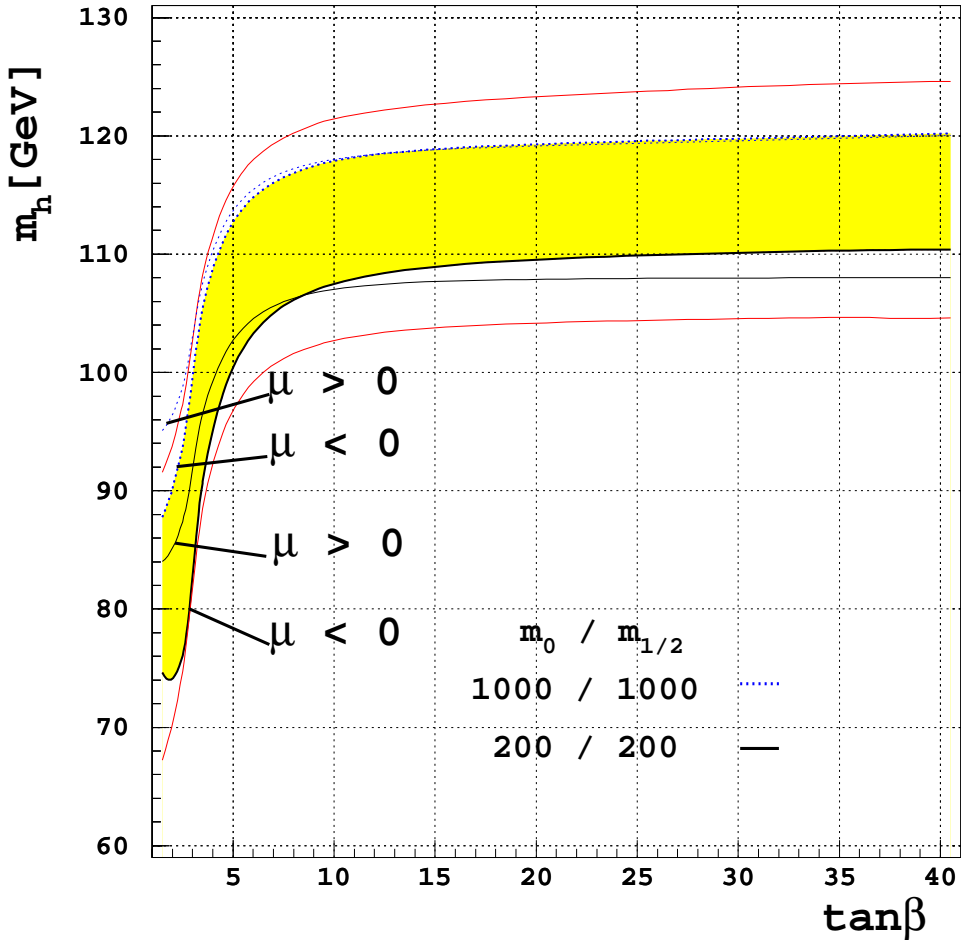


Figure 6: The dependence of the mass of the lighter \mathcal{CP} -even Higgs boson on $\tan\beta$, as calculated by the effective potential approach[21]. The shaded band shows the variation of $m_0 = m_{1/2}$ between 200 and 1000 GeV for $\mu < 0$, $m_t = 175$ GeV, and $A_0 = 0$. Note the small dependence on the sign of μ for large $\tan\beta$, as expected from the suppression of μ by $\tan\beta$ in the stop mixing. The maximum (minimum) Higgs boson mass value, shown by the upper (lower) line are obtained for $A_0 = -3m_0$, $m_t = 180$ GeV, $m_0 = m_{1/2} = 1000$ GeV ($A_0 = 3m_0$, $m_t = 170$ GeV, $m_0 = m_{1/2} = 200$ GeV). As can be seen the curves show an asymptotic behaviour for large values of $\tan\beta$.

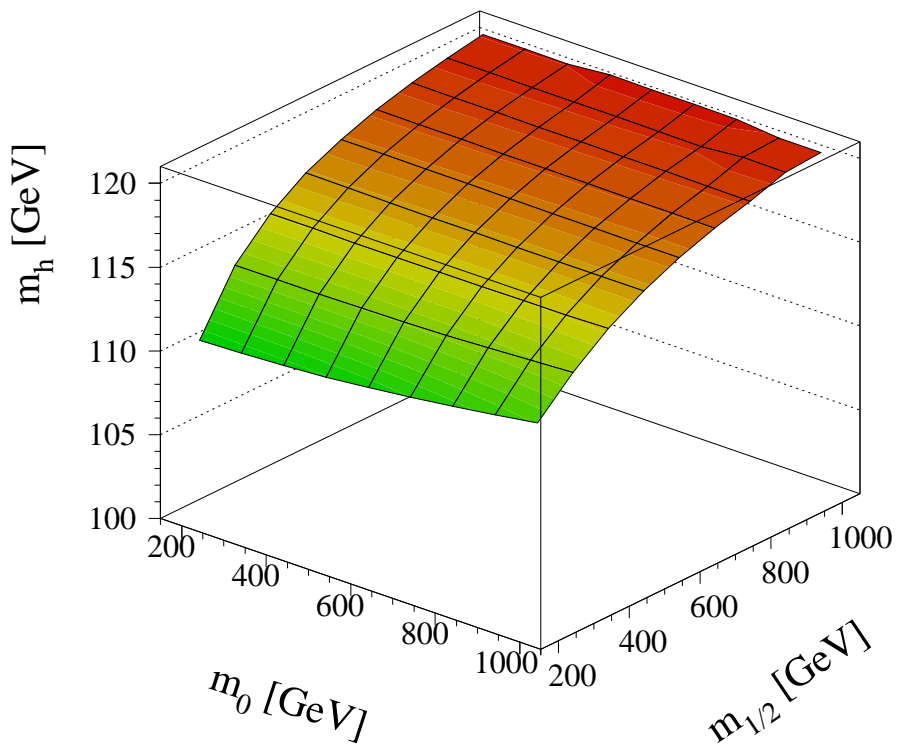


Figure 7: The Higgs boson mass as function as function of m_0 and $m_{1/2}$, as calculated by the effective potential approach[21].

$\tan\beta=35$

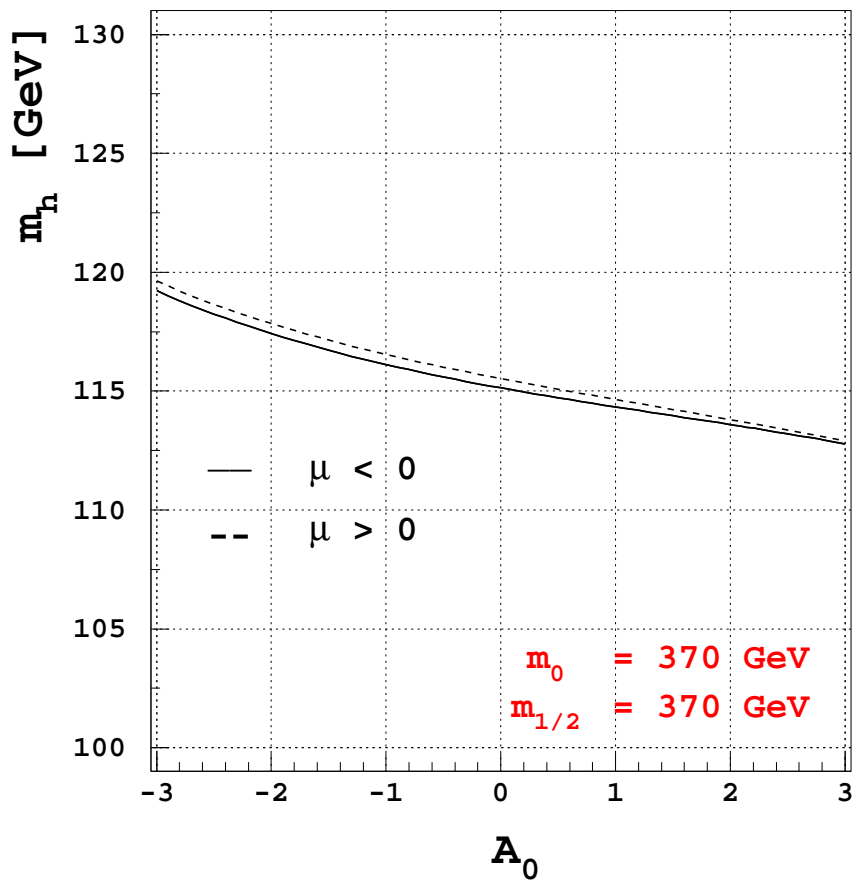


Figure 8: Dependence of the Higgs mass on the trilinear coupling A_0 at the GUT-scale in units of m_0 . The low-energy value A_t tends to a fixed point, thus reducing the influence of A_0 on the mixing in the stop sector.

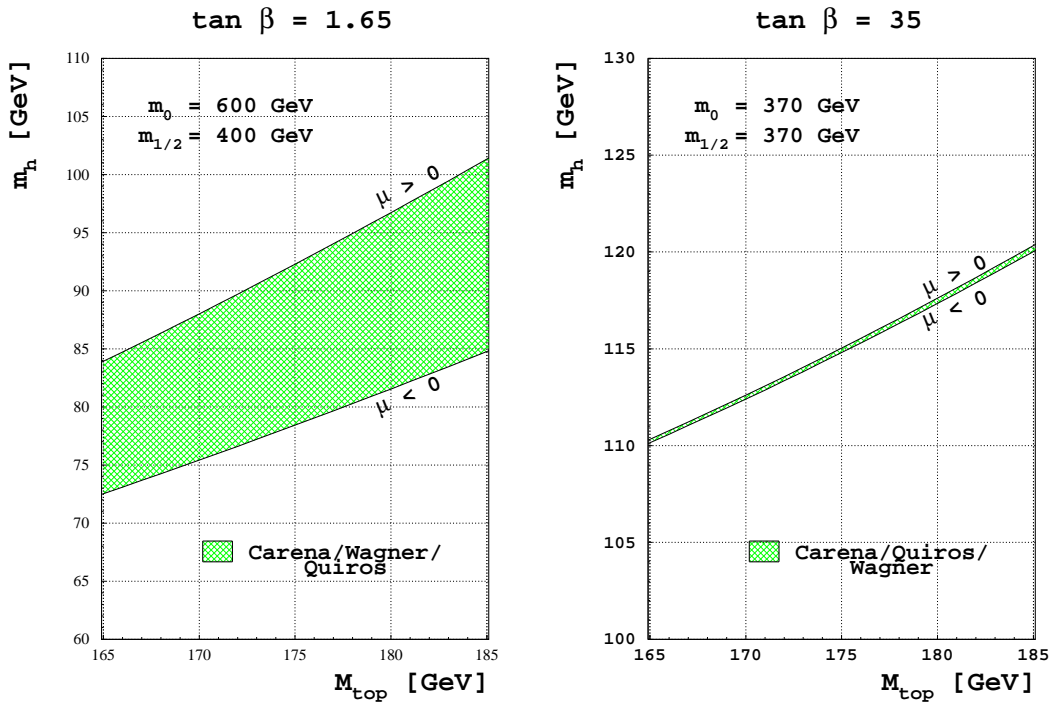


Figure 9: The top mass dependence of the Higgs mass in the low and high $\tan \beta$ scenario. Note the reduced dependence on the sign of μ for large $\tan \beta$, as expected from the stop mixing parameter $X_t = A_t - \mu/\tan \beta$.

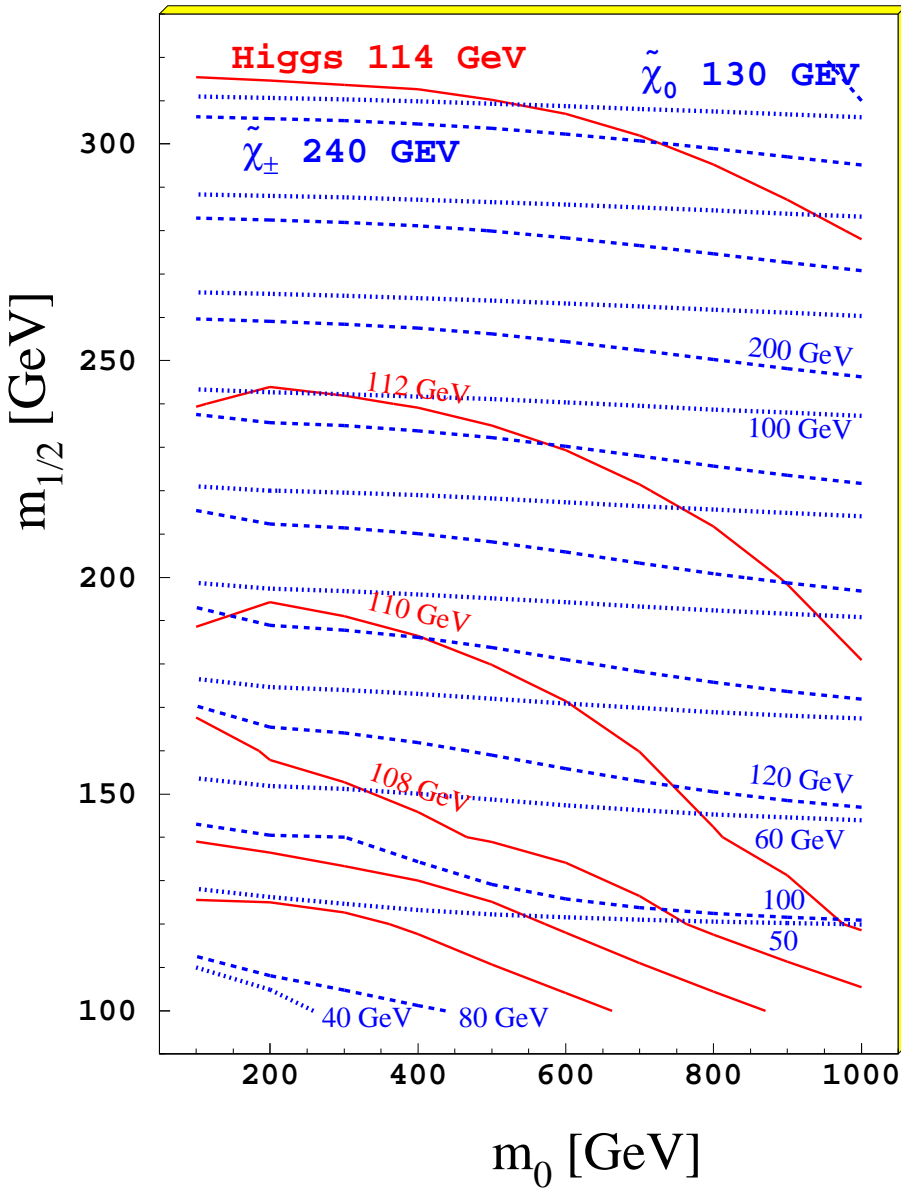


Figure 10: Contours of the Higgs mass (solid lines), lightest chargino mass (dashed) and LSP mass (fine dashed) in the $m_0, m_{1/2}$ plane in steps of 2,10 and 20 GeV. The region for a Higgs mass below 107.9 GeV and chargino mass below 100 GeV is excluded. It can be seen that an LSP mass of 52 GeV is excluded too, so the DAMA result interpreted as an LSP with a mass of 52^{+10}_{-8} [7] is at the edge of the allowed parameter space. This plot is for large $\tan\beta$; for smaller $\tan\beta$ the excluded region rapidly increases because of the Higgs mass limit.